

THE MASS PROFILE OF THE COMA GALAXY CLUSTER

M. J. Geller¹, Antonaldo Diaferio², and M. J. Kurtz¹

¹Harvard-Smithsonian Center for Astrophysics, 60 Garden St., Cambridge, MA 02138, USA

²Max-Planck-Institut für Astrophysik, Karl-Schwarzschild-Str. 1, D-85740, Garching, Germany

ABSTRACT

We use a new redshift survey complete to $m_R \simeq 15.4$ within 4.25° from the center of the Coma cluster to measure the mass profile of the cluster to $r \sim 5.5h^{-1}$ Mpc. We extend the profile to $r \sim 10h^{-1}$ Mpc with a further sample complete to $m_R = 15.4$ in 42% of the area within a 10° radius and to $m_{Zw} = 15.5$ in the remaining area. Galaxies within this region are falling onto the cluster on moderately radial orbits and thus do not satisfy virial equilibrium. Nonetheless, identification of the caustics in redshift space provides an estimate of the gravitational potential at radius r and hence of the system mass, $M(\leq 10h^{-1}\text{Mpc}) = (1.65 \pm 0.41) \times 10^{15}h^{-1}M_\odot$ ($1\text{-}\sigma$ error). Previous mass estimates derived from optical and X-ray observations are limited to $r \leq 2.5h^{-1}$ Mpc. Our mass profile is consistent with these estimates but extends to distances four times as large. Over the entire range, the mass increases with r at the rate expected for a Navarro, Frenk & White (1997) density profile.

Subject headings: dark matter — galaxies: clusters: individual (Coma) — methods: statistical — survey

1. INTRODUCTION

For more than sixty years, the Coma cluster has been the most widely studied system of galaxies (see the review by Biviano 1998). Zwicky (1933) first estimated the mass of a system of galaxies by applying the virial theorem to Coma. This measurement provided the first piece of evidence that dark matter dominates the gravitational dynamics of systems on megaparsec scales. More accurate analyses use the Jeans equation to include a surface term in the virial theorem which accounts for the unsampled portion of the system (The & White 1986). Major uncertainties in the mass arise from the assumption that light traces mass (The & White 1986; Merritt 1987). Alternatively, X-ray observations provide information about the gravitational potential of the cluster and therefore, by assuming hydrostatic equilibrium, the total mass profile (Hughes 1989; Watt et al. 1992; Hughes 1998). In spite of the assumptions involved, the mass determinations from optical and X-ray data in the core of the cluster ($r \lesssim 0.5h^{-1}$ Mpc) agree within a factor of two.

Although studies of the core of Coma are abundant, there are few quantitative studies of the outskirts (see e.g. the review by West 1998). These external regions are far from virial equilibrium

and therefore the data are more difficult to interpret. Furthermore, their large angular extent on the sky demands substantial amounts of telescope time for complete spectroscopic and photometric observations. Based on shallow (and often incomplete) redshift surveys, there have been analyses of this infall region to extract the value of the cosmological density parameter Ω_0 (Schectman 1982; Capelato et al. 1982; Regös & Geller 1989; van Haarlem et al. 1993). Alternatively, optical (Kent & Gunn 1982; Vedel & Hartwick 1998) and X-ray data (Hughes 1989; Makino 1994) have been extrapolated to obtain a mass estimate at $r \sim 3h^{-1}$ Mpc.

Galaxies falling into the potential well of a cluster populate a well-defined region in redshift space. Diaferio & Geller (1997) show that, in hierarchical clustering scenarios, the amplitude of the caustics which bound this region is proportional to the gravitational potential of the dark matter halo. In fact, because clusters accrete mass through the aggregation of smaller systems, random motions rather than spherical infall determine the amplitude of the caustics. Thus, measurement of the amplitude of the caustics yields the system mass, as long as galaxies trace the velocity field of the infall region reliably. This argument applies at radii as large as $\sim 10h^{-1}$ Mpc. N -body simulations of Cold Dark Matter models which include a semi-analytic treatment of galaxy formation and evolution suggest that there is no velocity bias on the relevant scales (Kauffmann et al. 1999; Diaferio et al. 1999). Diaferio (1999) uses these simulations to show that the mass estimation technique we apply here yields estimates to $r = 5-10h^{-1}$ Mpc with a typical uncertainty of 50% for samples of a few hundred galaxies.

As a first application of the mass estimation technique, we use a new redshift survey covering the Coma cluster to a 10° radius to measure the cluster mass profile. The largest of our samples contains 1693 redshifts. We briefly describe the redshift survey (Sect. 2), outline the mass estimation technique (Sect. 3), and discuss the results (Sect. 4).

2. THE DATA

To explore the infall region surrounding the Coma cluster we measured 447 new redshifts for galaxies with $m_R \leq 15.4$ within 4.25° of the center of the Coma cluster and in a strip between $26.5^\circ < \delta_{1950} < 32.5^\circ$. Our redshift survey is complete to $m_R = 15.4$ within 4.25° of the cluster center. Within 10° of the cluster center the survey is complete to $m_R = 15.4$ for 42% of the area and to $m_{Zw} = 15.5$ for the remaining area.

We measured redshifts with the FAST spectrograph on the 1.5-meter telescope at Whipple Observatory. The FAST observations are typically 5-20 minute exposures with a 300 line mm^{-1} grating, providing spectral coverage from 3600–7600Å at 6Å resolution. We use the IRAF task XCSAO in the RVSAO package (Kurtz and Mink 1998) to determine radial velocities based on absorption- and emission-line template cross-correlation. We compute the uncertainties in the velocities according to the procedures in Kurtz and Mink (1998).

We identified galaxies brighter than $m_R = 15.4$ from Space Telescope Institute scans of the

POSS E plates (provided by B. McLean and M. Postman). We calibrated the instrumental magnitudes by comparison with the Century Survey (Geller et al. 1997). For each plate in the strip (5 plates) we fit the zero point offset and the non-linear scale error. For plate E1393, which contains the cluster center, we also calibrated against the CCD photometry of Kashikawa et al. (1998). For the Century Survey calibrators we obtained a zero point offset (at $R = 15.0$) of -0.13 mag and a slope for the scale error of -0.228 mag/mag; the Kashikawa calibrators yielded -0.16 and -0.223 , respectively. We estimate that the magnitude limit is uncertain by $\sim 0.1^m$. The catalog to a radius of 10° contains all of the galaxies in the Zwicky (Zwicky & Herzog 1963) catalog with $m_{Zw} \leq 15.5$.

We consider three different samples: (1) L4.25: 485 galaxies brighter than $m_R = 15.4$ within a 4.25° radius; (2) L10.0: 1077 galaxies with $m_R \leq 15.4$ or $m_{Zw} \leq 15.5$ within a 10° radius; and (3) C10.0: a compilation of 1693 galaxies within 10.0° regardless of their apparent magnitude. The C10.0 sample includes redshifts from Thorstensen et al. (1989), Wegner et al. (1990), Huchra et al. (1992), Thorstensen et al. (1995), van Haarlem et al. (1993), Colless & Dunn (1996), Geller et al. (1997), Falco et al. (1999).

3. MASS PROFILE

In redshift space, galaxies around clusters appear within regions delimited by caustics with a characteristic trumpet shape (Kaiser 1987): outside the caustics, the density of galaxies drops substantially. Galaxies outside the caustics are background or foreground galaxies (e.g. den Hartog & Katgert 1996).

Half of the redshift space distance between the upper and the lower caustic at projected separation r from the cluster center defines the amplitude $\mathcal{A}(r)$. If we assume spherical symmetry, $\mathcal{A}(r)$ is a measure of the gravitational potential $\phi(r)$. We can thus estimate the cluster mass profile from the inner halo to the outer infall regions. In spite of the assumption of spherical symmetry, the technique yields mass profiles accurate to $\sim 50\%$ for a suite of N -body simulations (Diaferio & Geller 1997; Diaferio 1999).

We now apply the mass estimation technique described in Diaferio (1999) to Coma. To derive a cluster center and velocity, a hierarchical cluster analysis identifies the cluster members. An adaptive kernel method locates the peak of the density distribution of the cluster members on the plane of the sky; the cluster redshift is the median of the cluster member velocity distribution. In the cleanly magnitude limited sample L4.25, we identify 263 cluster members. The center we derive for Coma is $\alpha_c(2000) = 12^{\text{h}}59^{\text{m}}25.0^{\text{s}}$, $\delta_c(2000) = 27^\circ56'45.7''$, and $cz_c = 7090$ km s $^{-1}$. This position differs by a few arcminutes and by ~ 250 km s $^{-1}$ from, for example, the center of the main condensation in Coma identified by Colless and Dunn (1996). The meaning of our center is not quite the same as earlier optical and X-ray determinations; ours is an estimate of the minimum of the global Coma system potential well derived from a more extended survey than available heretofore. We use the same center for all of the samples we analyze.

At the threshold in the binary tree used to identify the cluster members, there are a number of groups distinct from the main cluster. We use the procedure applied to the whole cluster to determine the center of each group. We then limit our analysis to individual galaxies, i.e. galaxies that do not belong to any group, and to galaxies in groups which lie within $cz_{\max} = 4000 \text{ km s}^{-1}$ of the cluster center. Larger values of cz_{\max} do not change our results; galaxies at these redshift distances have no effect on the location of the caustics. Smaller values might exclude galaxies in the cluster core. We locate all galaxies in the redshift diagram (r, v) , where

$$r = \frac{cz_c}{H_0} \sin \theta; \quad v = cz - cz_c \cos \theta. \quad (1)$$

Here, cz_c , cz , and θ are the redshift of the cluster center, the galaxy redshift and the angular separation between the cluster center and the galaxy, respectively.

We now use an adaptive kernel method to compute the two-dimensional density distribution $f_q(r, v)$ of the galaxies within the redshift diagram. To compute $f_q(r, v)$ with a spherical smoothing window, we rescale r and v so that the ratio h_v/h_r of the smoothing window sizes along v and r respectively is $q = 25$. This choice yields equal weight to the typical uncertainties on v and r , e.g. 50 km s^{-1} and $0.02h^{-1} \text{ Mpc}$ for nearby clusters, respectively. Different values of q in the range [10, 50] have negligible effects on the results. We then identify the threshold κ which minimizes the quantity

$$S(\kappa, R) = |\langle v_{\text{esc}}^2 \rangle_{\kappa, R} - 4\langle v^2 \rangle_R|^2, \quad (2)$$

where $\langle v^2 \rangle_R$ is the velocity dispersion of the cluster members and $\langle v_{\text{esc}}^2 \rangle_{\kappa, R}$ is the escape velocity computed with the estimated $\mathcal{A}(r)$; $R = 1.16h^{-1} \text{ Mpc}$ is the mean distance of the cluster members from the cluster center. We compute the caustic amplitude $\mathcal{A}(r) = \min\{v_u(r), v_d(r)\}$ where $v_u(r)$ and $v_d(r)$ are the solutions of the equation $f_q(r, v) = \kappa$.

The mass $M(< r)$ within the radius r from the cluster center is

$$GM(< r) = \frac{1}{2} \int_0^r \mathcal{A}^2(x) dx. \quad (3)$$

To quantify the error in the amplitude and the mass profile, we assume that the relative error $\delta\mathcal{A}(r)/\mathcal{A}(r) = \kappa/\max\{f_q(r, v)\}$ and $\delta M_i = \sum_{j=1, i} |2m_j \delta\mathcal{A}(r_j)/\mathcal{A}(r_j)|$, where m_j is the mass of the shell $[r_{j-1}, r_j]$

$$Gm_j = \frac{1}{2} \int_{r_{j-1}}^{r_j} \mathcal{A}^2(x) dx. \quad (4)$$

N -body simulations show that this expression approximates the $1\text{-}\sigma$ spread of profiles obtained by projecting the clusters along different lines of sight.

The upper panels of Figure 1 show the redshift diagrams of Coma for our three samples. Each case shows a clearly defined high density region around the median redshift of Coma. The bold lines show where our method locates the caustics. Variations of $\mathcal{A}(r)$ from sample to sample are within the $3\text{-}\sigma$ uncertainty (middle panels). Thus, the mass profile (eq. [3]) is also consistent from

sample to sample. The shaded areas in the middle and bottom panels show the $2\text{-}\sigma$ uncertainty of the profiles. Because our three samples contain galaxies of different luminosity, the consistency of the profiles indicates that (1) galaxies are tracers and that (2) velocity bias is negligible as we have assumed.

We limit our profile to $r = 10h^{-1}$ Mpc. At larger distances, the meaning of a “cluster” is unclear. Our largest sample indicates $M(\leq 5.5h^{-1}\text{Mpc}) = (1.44 \pm 0.29) \times 10^{15}h^{-1}M_{\odot}$ and $M(\leq 10h^{-1}\text{Mpc}) = (1.65 \pm 0.41) \times 10^{15}h^{-1}M_{\odot}$ ($1\text{-}\sigma$ error). Error bars in Figure 1 show the range of X-ray mass estimates available at $r = 0.5h^{-1}$ Mpc and $r = 2.5h^{-1}$ Mpc (Hughes 1989). At these small radii, our estimate agrees very well with the X-ray estimates.

We also plot the cumulative mass profile for a softened isothermal sphere (short-dashed line) and for a halo with a Navarro, Frenk & White (1997; NFW) profile (long-dashed line). We fit these respective mass profiles $M(< r) = 4\pi\rho_0r_c^3[(r/r_c) - \arctan(r/r_c)]$ and $M(< r) = 4\pi\delta_c\rho_c r_s^3\{\log[1 + (r/r_s)] - (r/r_s)/[1 + (r/r_s)]\}$ in the range $r = [0, 1]h^{-1}$ Mpc; ρ_0 , r_c , δ_c and r_s are fitting parameters, and $\rho_c = 3H_0^2/8\pi G$ is the critical density of the Universe. For the NFW profile we find $r_s = 0.182 \pm 0.030$, 0.167 ± 0.029 , and $0.192 \pm 0.035h^{-1}$ Mpc for the L4.25, L10.0, and C10.0 sample, respectively. Note that larger fit ranges, up to $r = [0, 5]h^{-1}$ Mpc, do not change r_s . The softened isothermal sphere yields a poor fit for any fit range larger than $r = [0, 2]h^{-1}$ Mpc. The fit parameters determine the expected behavior of the profiles at larger radii. Our measurement shows clearly that the NFW extrapolation agrees remarkably well with the observed mass increase. The mass profile for the isothermal sphere increases too steeply for consistency with the data.

The parameter δ_c in the NFW profile is related to the concentration parameter $c = r_{200}/r_s$, where r_{200} is the radius of the sphere with average mass density 200 times the critical density. We can therefore estimate the virial radius r_{200} of Coma: we find $r_{200} \simeq 1.5h^{-1}$ Mpc for each of our three samples.

4. DISCUSSION

We use a redshift survey within 10° of the center of the Coma cluster to measure the mass profile of the cluster to $r = 10h^{-1}$ Mpc: $M(\leq 10h^{-1}\text{Mpc}) = (1.65 \pm 0.41) \times 10^{15}h^{-1}M_{\odot}$ ($1\text{-}\sigma$ error). This mass profile extends to distances 50 times larger than the cluster core radius $r_s \sim 0.2h^{-1}$ Mpc and to substantially larger radius than previous estimates. The mass profile appears robust: it does not change appreciably when we increase the size of the dataset.

The mass profile increases at a rate consistent with the NFW density profile and substantially smaller than the density profile for an isothermal sphere. Because the NFW mass profile increases only logarithmically, our results do not exclude convergence of the mass of Coma at $r \gtrsim 3 - 4h^{-1}$ Mpc. However, the agreement between our measurement and the increasing NFW profile does suggest that, other than a density contrast criterion, there is no obvious definition of the extent of the halo of Coma. We can use the NFW density profile fit to estimate the virial radius of Coma

$$r_{200} = 1.5h^{-1} \text{ Mpc.}$$

Geller et al. (1999) will include the data, an analysis of the substructure within the infall region of Coma, and a discussion of the morphologies and spectroscopic properties of galaxies in the infall region. In forthcoming papers, we will apply our mass estimation technique to similar data obtained for the infall regions of the Abell clusters A539, A576 and A1367 and for the A2199/A2197 double cluster.

The mass estimation method we apply here depends on kinematic data only. If velocity biases are weak, as suggested by high resolution N -body simulations including a phenomenological treatment of galaxy formation (Kauffmann et al. 1999; Diaferio et al. 1999), the mass estimate is independent of the luminosity distribution: with accurate photometric data we can then measure the behavior of the mass-to-light ratio out to $\sim 5 - 10h^{-1}$ Mpc scale. In the future we hope to report such a measurement for the Coma cluster.

From photometric data, we can also quantify the variation of the galaxy population and its kinematic properties with the distance from the cluster center. Within the virial radius of clusters the fraction of blue galaxies increases with radius (Dressler 1980; Whitmore & Gilmore 1992; Carlberg et al. 1997; de Theije & Katgert 1999) and their velocity dispersion is generally larger than the velocity dispersion of red galaxies (Mohr et al. 1996; Carlberg et al. 1997), indicating that blue galaxies are actually falling into the cluster and do not satisfy virial equilibrium (e.g. Biviano et al. 1997). N -body simulations of Cold Dark Matter models naturally reproduce these properties (Diaferio et al. 1999). These simulations also show that kinematic differences between blue and red galaxies become smaller at radii larger than the virial radius, but at different rates in universes with different Ω_0 . Therefore, by combining photometric and spectroscopic data covering the infall regions of galaxy clusters over a large redshift range we can potentially discriminate among cosmological models.

We thank Perry Berlind and Michael Calkins for measuring the redshifts at the Whipple Observatory 1.5-meter, Susan Tokarz for reduction of the spectroscopic data, Brian McLean and Marc Postman for providing galaxy positions from the Space Telescope Institute POSS scans. We also thank Peter Schneider, Ravi Sheth, Bepi Tormen, Simon White and Saleem Zaroubi for fruitful discussions and an anonymous referee for relevant suggestions. During this project, A.D. was a Marie Curie Fellow and held grant ERBFMBICT-960695 of the Training and Mobility of Researchers program financed by the European Community. A.D. also acknowledges support from an MPA guest post-doctoral fellowship. M.J.G. and M.J.K. acknowledge support from the Smithsonian Institution.

REFERENCES

- Biviano, A. 1998, in *Untangling Coma Berenices: A New Vision of an Old Cluster*, ed. A. Mazure, F. Casoli, F. Durret, & D. Gerbal, (Singapore: Word Scientific), 1
- Biviano, A., Katgert, P., Mazure, A., Moles, M., den Hartog, R., Perea, J., & Focardi, P. 1997, *A&A*, 321, 84
- Capelato, H. V., Gerbal, D., Mathez, G., Mazure, A., & Salvador-Solé, E. 1982, *ApJ*, 252, 433
- Carlberg, R. G. et al. 1997, *ApJ*, 476, L7
- Colless, M., & Dunn, A. M. 1996, *ApJ*, 458, 435
- de Theije, P. A. M., & Katgert, P. 1999, *A&A*, 341, 371
- den Hartog, R., & Katgert, P. 1996, *MNRAS*, 279, 349
- Diaferio, A. 1999, *MNRAS*, submitted
- Diaferio, A., & Geller, M. J. 1997, *ApJ*, 481, 633
- Diaferio, A., Kauffmann, G., Colberg, J. M., & White, S. D. M. 1999, *MNRAS*, submitted
- Dressler, A. 1980, *ApJ*, 236, 351
- Falco, E.E., Kurtz, M.J., Geller, M.J., Huchra, J.P., Peters. J., Berlind, P., Mink, D.J., Tokarz, S.P. & Elwell, B. 1999, *PASP*, in press (April 1)
- Geller, M. J., et al. 1997, *AJ*, 114, 2205
- Geller, M. J., et al. 1999, in preparation
- Huchra, J.P., Geller, M.J., Clemens, C.M., Tokarz, S.P. & Michel, A. 1992, *B.I. CDS* 41, 31
- Hughes, J. P. 1989, *ApJ*, 337, 21
- Hughes, J. P. 1998, in *Untangling Coma Berenices: A New Vision of an Old Cluster*, ed. A. Mazure, F. Casoli, F. Durret, & D. Gerbal, (Singapore: Word Scientific), 175
- Kashikawa, N., Sekiguchi, M., Doi, M., Komiyama, Y., Okamura, S. Shimasaku, K., Yagi, M. & Yasuda, N. 1998, *ApJ*, 500, 750.
- Kaiser, N. 1987, *MNRAS*, 227, 1
- Kauffmann, G., Colberg, J. M., Diaferio, A., & White, S. D. M. 1999, *MNRAS*, 303, 188
- Kent, S. M., & Gunn, J. E. 1982, *AJ*, 87, 945
- Kurtz, M. J., & Mink, D. J. 1998 *PASP*, 110, 934

- Makino, N. 1994, PASJ, 46, 139
- Merritt, D. 1987, ApJ, 313, 121
- Mohr, J. J., Geller, M. J., Fabricant, D. G., Wegner, G., Thorstensen, J., & Richstone, D. O. 1996, ApJ, 470, 724
- Navarro, J. F., Frenk, C. S., & White, S. D. M. 1997, ApJ, 490, 493
- Regös, E., & Geller, M. J. 1989, AJ, 98, 755
- Schectman, S. A. 1982, ApJ, 262, 9
- The, L. S., & White, S. D. M. 1986, AJ, 92, 1248
- Thorstensen, J.R., Wegner, G.A., Hamwey, R., Boley, F., Geller, M.J., Huchra, J.P. Kurtz, M.J. & Mc Mahan, R.K. 1989, AJ, 98, 1143
- Thorstensen, J.R., Kurtz, M.J., Geller, M.J., Ringwald, F. & Wegner, G. 1995, AJ, 109, 2368
- van Haarlem, M. P., Cayón, L., Gutiérrez de la Cruz, C., Martínez-González, E., & Rebolo, R. 1993, MNRAS, 264, 71
- Vedel, H., & Hartwick, F. D. A. 1998, ApJ, 501, 509
- Watt, M. P., Ponman, T. J., Bertram, D., Eyles, C. J., Skinner, G. K., & Willmore, A. P. 1992, MNRAS, 258, 738
- Wegner, G.A., Thorstensen, J.R., Kurtz, M.J., Geller, M.J., & Huchra, J. P. 1990, AJ, 100, 1405.
- West, M. J. 1998, *Untangling Coma Berenices: A New Vision of an Old Cluster*, ed. A. Mazure, F. Casoli, F. Durret, & D. Gerbal, (Singapore: Word Scientific), 36
- Whitmore, B. C., & Gilmore, D. M. 1992, ApJ, 367, 64
- Zwicky, F. 1933, *Helv. Phys. Acta*, 6, 110
- Zwicky, F. & Herzog, E. *Catalogue of galaxies and clusters of galaxies*, (Pasadena: California Institute of Technology) Vol III

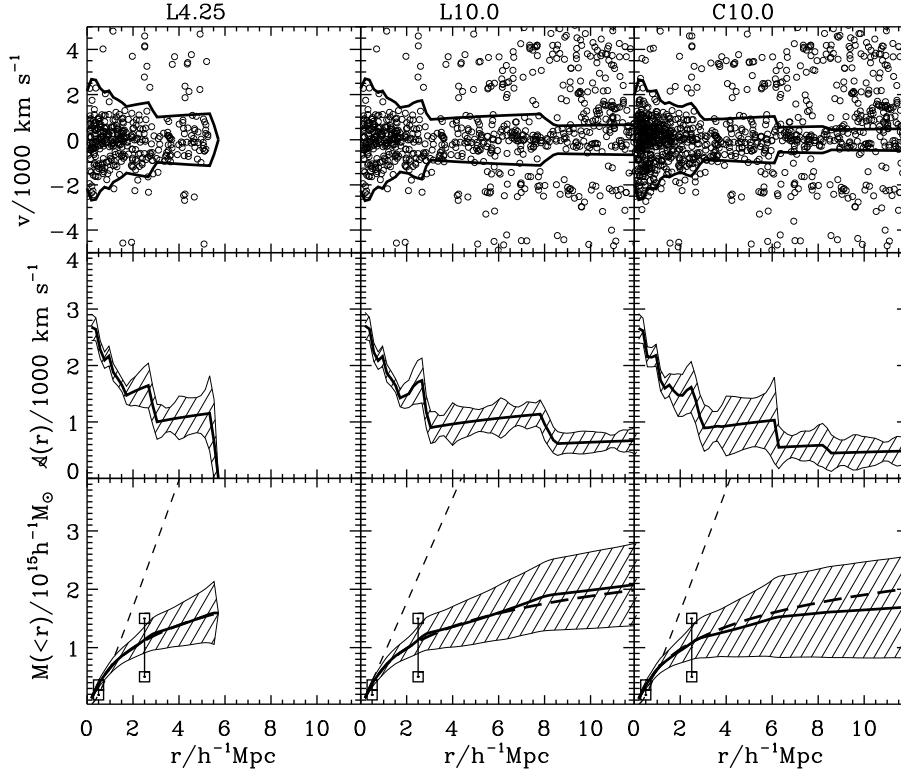


Fig. 1.— **Top panels:** Galaxy distribution in the redshift diagram for our three samples. The bold lines indicate the location of the caustics. There are 332, 480, and 691 galaxies within the caustics in the samples L4.25, L10.0, and C10.0, respectively. Half the distance between the caustics defines the amplitude $A(r)$ shown in the middle panels. **Bottom panels:** The bold lines are the mass profiles derived from the data with eq. (3). The two error bars show the range of the X-ray mass estimates listed in Hughes (1989). Short-dashed and long-dashed lines are the cumulative mass profile for a softened isothermal sphere and an NFW density profile with parameters obtained by fitting the mass profile in the range $[0, 1]h^{-1} \text{ Mpc}$. Shaded areas in the middle and bottom panels indicate the $2\text{-}\sigma$ uncertainty.